A Novel High-Performance Strategy for A Sensorless AC Motor Drive

Dong-Hee Lee and Young-Ahn Kwon

Abstract - The sensorless AC motor drive is a popular topic of study due to the cost and reliability of speed and position sensors. Most sensorless algorithms are based on the mathematical modeling of motors including electrical variables such as phase current and voltage. Therefore, the accuracy of such variables largely affects the performance of the sensorless AC motor drive. However, the output voltage of the SVPWM-VSI, which is widely used in sensorless AC motor drives, has considerable errors. In particular, the SVPWM-VSI is error-prone in the low speed range because the constant DC link voltage causes poor resolution in a low output voltage command and the output voltage is distorted due to dead time and voltage drop. This paper investigates a novel high-performance strategy for overcoming these problems in a sensorless ac motor drive. In this paper, a variation of the DC link voltage and a direct compensation for dead time and voltage drop are proposed. The variable DC link voltage leads to an improved resolution of the inverter output voltage, especially in the motor's low speed range. The direct compensation for dead time and voltage drop directly calculates the duration of the switching voltage vector without the modification of the reference voltage and needs no additional circuits. In addition, the proposed strategy reduces a current ripple, which deteriorates the accuracy of a monitored current and causes torque ripple and additional loss. Simulation and experimentation have been performed to verify the proposed strategy.

Keywords - sensorless AC motor drive, SVPWM, variable link voltage, dead time compensation, current ripple

1. Introduction

Variable-speed drives are being continually improved. The sensorless ac motor drive has recently been a popular topic of study due to its several advantages [1-3]. Most sensorless algorithms are based on the mathematical modeling of motors including electrical variables such as phase current and voltage. Therefore, the accuracy of such variables largely affects the performance of the sensorless ac motor drive. The SVPWM-VSI (Space Vector Pulse Width Modulation of Voltage Source Inverter) is widely used for high performance of variable-speed sensorless AC motor drives but the output voltage of the SVPWM-VSI supplying a motor has a considerable error because it is distorted by a variety of sources. Most studies for improving performance of the SVPWM-VSI have concentrated on switching pattern and dead time compensation [4-9]. However, a constant DC link voltage that is appropriately fixed to the rated load causes a large voltage error and current ripple in the low speed range of a motor because it has poor resolution in a low output voltage command of the SVPWM-VSI, that is, in a low speed command. In addition, a current ripple produced in the SVPWM-VSI deteriorates the accuracy of a monitored current and causes torque ripple and additional loss.

This paper investigates a novel high-performance strategy for overcoming these problems in a sensorless AC motor drive . In this paper, a variation of the DC link voltage and direct compensation for dead time and voltage drop are proposed for an improved output voltage. The variable DC link voltage improves the resolution of the output voltage of the SVPWM-VSI, especially in a low output voltage command. The direct compensation for dead time and voltage drop directly calculates the duration of the switching voltage vector without the modification of the reference voltage and needs no additional circuits. In addition, the proposed strategy has an advantage of reducing a current ripple produced in the SVPWM-VSI. The proposed strategy is verified through simulation and experimentation which are performed in a sensorless AC motor drive.

2. The Sensorless AC Motor Drive

Sensorless drives eliminate additional mounting space, increase the reliability in harsh environments, and reduce the cost of the motor. Recently, various sensorless algorithms of the ac motor drive have been proposed for the elimination of speed and position sensors: estimators using state equations, model reference adaptive systems, Luenberger or Kalman observers, direct control of torque and flux, artificial intelligence, saliency effects, and so on. Most sensorless algorithms are based on the mathe-

This work was supported by grant no. R05-2000-000-00267-0 from the Basic Research Program of the Korea Science & Engineering Foundation.
Manuscript received: March 15, 2002 accepted June 26, 2002
Dong-Hee Lee and Young-Ahn Kwon are with the School of Electrical Engineering, Pusan National University, Pusan, Korea.

matical modeling of motors, and all the information is obtained by utilizing the monitored voltages and currents [3]. Therefore, the accuracy of such variables largely affects the performance of the sensorless AC motor drive.

Fig. 1 shows the block diagram of a variable-speed sensorless AC motor drive. The terminal currents are directly measured from a motor, but terminal voltages are not directly monitored because of switching noise. The motor voltages, which are obtained from the command voltage, are substituted for the terminal voltages. However, the output voltage of the SVPWM-VSI supplying a motor has a considerable error, especially in a low speed range. A constant DC link voltage that is appropriately fixed to the rated load has a poor resolution in a low speed range, and the inverter output voltage is distorted due to dead time and voltage drop. In addition, a current ripple produced in the SVPWM-VSI deteriorates the accuracy of a monitored current and causes torque ripple and additional loss. This study concentrated on solving these problems to obtain high performance of sensorless ac motor drive.

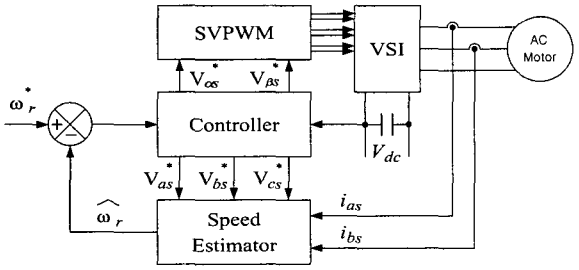

Fig. 1 Block diagram of variable-speed sensorless drive

3. The SVPWM-VSI

3.1 SVPWM switching scheme

Fig. 2 shows a three-phase VSI connected to an AC motor. Currently, SVPWM of inverter switches is widely used for high performance of a variable-speed sensorless AC motor drive. Various SVPWM techniques have been studied due to the advantages of low harmonic distortion and high modulation ratio of the DC link voltage compared to other PWMs [4-6].

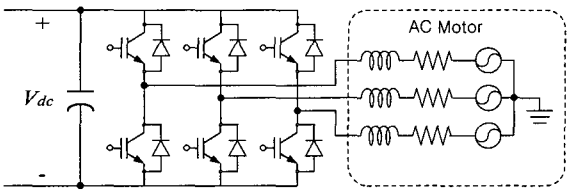

Fig. 2 A simple diagram of three-phase VSI

From the eight switching states of the VSI, six effective (non-zero) and two zero voltage vectors are possible as shown in Fig. 3(a). Two zero voltage vectors are associated with the states of the upper three switches closed or the lower three switches closed. Magnitudes of six effective and two zero voltage vectors are $2/3\,V_{dc}$ and zero, respectively. A certain voltage vector may be obtained by the combination of switching voltage vectors.

Therefore, a switching pulse pattern of inverter switches is determined from the combination of switching voltage vectors, and several combinations are possible.

The reference voltage of each phase may be written as follows if the reference voltages of three phases are sorted by magnitude.

$$V_{MAX}^{*} = \frac{2}{3} V_{dc} \frac{T_1}{T_S} + \frac{1}{3} V_{dc} \frac{T_2}{T_S} \quad (1)$$

$$V_{MID}^{*} = -\frac{1}{3} V_{dc} \frac{T_1}{T_S} + \frac{1}{3} V_{dc} \frac{T_2}{T_S} \quad (2)$$

$$V_{MIN}^{*} = -\frac{1}{3} V_{dc} \frac{T_1}{T_S} - \frac{2}{3} V_{dc} \frac{T_2}{T_S} \quad (3)$$

$$V_{MAX}^{*} + V_{MID}^{*} + V_{MIN}^{*} = 0 \quad (4)$$

where T_S is the sampling period and T_1, T_2, T_O are the durations of effective and zero voltage vectors.

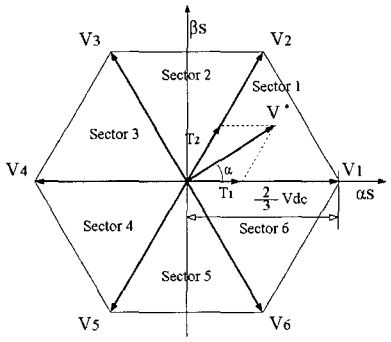

(a) Switching voltage vectors

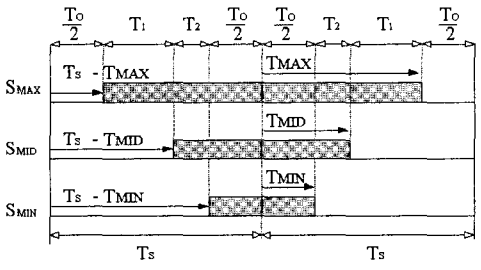

(b) Switching pulse pattern

Fig. 3 Switching voltage vectors and pulse pattern of the SVPWM-VSI

The SVPWM switching scheme may be easily implemented by a simple sorting of reference voltages as

shown in Eqs. (1) - (3) [10].

From Eqs. (1) - (3), the durations of switching voltage vectors are obtained as follows :

$$T_1 = (2\,V_{MAX}^* + V_{MIN}^*)\frac{T_S}{V_{dc}} \quad (5)$$

$$T_2 = -(V_{MAX}^* + 2\,V_{MIN}^*)\frac{T_S}{V_{dc}} \quad (6)$$

$$T_O = T_S - (T_1 + T_2) \quad (7)$$

From Eqs. (5) - (7), the switch-on duration of the upper switch of each phase may be determined as

$$T_{MAX}^* = T_O/2 + T_1 + T_2 \quad (8)$$

$$T_{MID}^* = T_O/2 + T_2 \quad (9)$$

$$T_{MIN}^* = T_O/2 \quad (10)$$

From Eqs. (8) - (10), the switch-on durations of the upper switches, T_{MAX}^*, T_{MID}^* and T_{MIN}^*, are directly calculated from T_1, T_2 and T_0. Fig. 3(b) shows the switching pulse pattern where S_{MAX}^*, S_{MID}^* and S_{MIN}^* mean phase switching signals that are sorted by magnitude.

3.2 Output voltage resolution

The switch-on duration of inverter switches obtained in Section 3.1 may not be exactly realized because the switching time of the switching voltage vector is determined by the subsampling frequency (resolution frequency) as shown in Fig. 4. In this figure, T_{ga}^* is the calculated switching time, and t_{ga} is the actual switching time. This difference causes an output voltage error, which is serious in a low output voltage command of the SVPWM-VSI. Figs. 5(a) and 5(b) show output voltage errors due to voltage resolution where the frequency of a reference output voltage is 6.667 Hz and the sampling period is 100 μs. It is assumed that an output voltage error may be largely reduced if the ratio V_{ref}^*/V_{dc} is appropriately controlled and is located in the normal range.

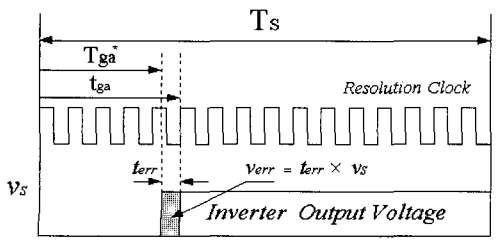

Fig. 4 Calculated and actual switching times

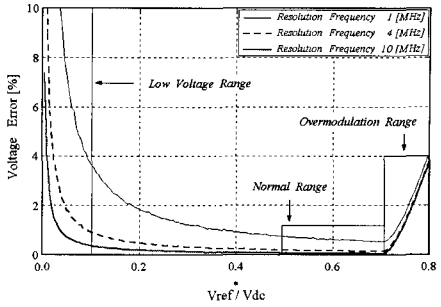

(a) The ratio V_{ref}^*/V_{dc} changed

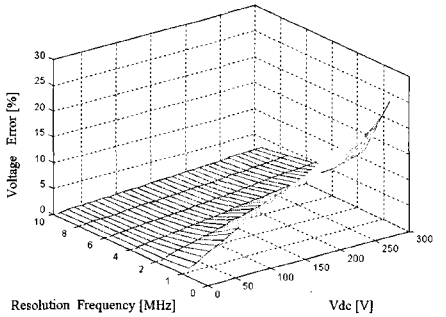

(b) V_{ref}^*=5V and V_{dc} changed

Fig. 5 Output voltage error due to voltage resolution

3.3 Dead time and voltage drop

The output voltage of the SVPWM-VSI has an error due to dead time and voltage drop. Dead time is always required to avoid short circuiting of the two switches in each leg of the inverter and is chosen to be a few microseconds for a fast switching device. Voltage drop is due to a forward voltage across the switching device in the on state. Fig. 6 shows the effect of dead time in the SVPWM-VSI. The current waveforms are obtained from a computer simulation which is performed in dead times of zero and 10 μs. Output voltage is $10/\sqrt{2}$ V, V_{dc} is 20 V in no dead time, and V_{dc} are 20 V and 100 V in 10 μs dead time. The dead time effect is large in a high DC link voltage, and many studies have pursued its compensation [7-10].

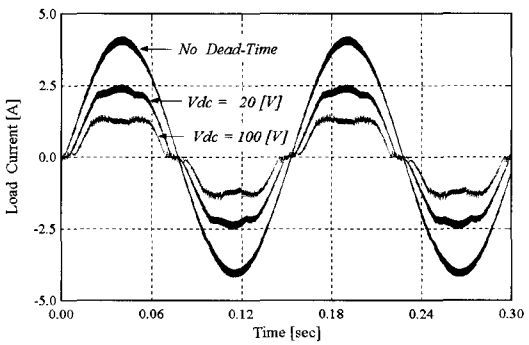

Fig. 6 Dead time effect in the SVPWM-VSI

4. Proposed Strategy

4.1 Variable DC link voltage

To reduce an output voltage error due to voltage resolution, a variable DC link voltage system is proposed. In this system, DC link voltage is appropriately controlled according to the reference output voltage of the SVPWM-VSI. Variable DC link voltage may be implemented by several topologies [11,12]. In this paper, a simple and well-known Buck converter is utilized as shown in Fig. 7.

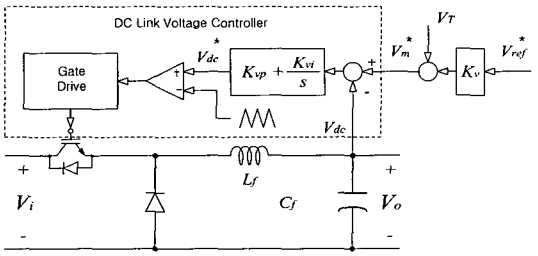

Fig. 7 Variable DC link voltage system

The DC link voltage should remain at or above a certain value so that the system may be stable. Therefore, the modified reference voltage may be written as follows and may be realized by using a feedback control as shown in Fig. 7.

$$V_m^* = k_v V_{ref}^* + V_T \tag{11}$$

where k_v is the proportional constant, V_T is the limit value of DC link voltage, and V_{ref}^* ($= \sqrt{V_{ds}^* + V_{qs}^*}$) is the command voltage calculated in sensorless controller.

The limit value of the DC link voltage is determined for the stable performance of variable DC link voltage system and is 5 V in this paper. In addition, the variable DC link voltage has an advantage of reducing a current ripple produced in the SVPWM-VSI and of reducing torque ripple and additional loss due to current ripple. This effect is well shown in Figs. 8(a) and 8(b), which are the current ripples produced in DC link voltages of 300 V and 15 V and in one sampling period of 200 μ s. The shadowed parts of Fig. 8 are the voltages applied to the phase winding of a motor, and the voltages have the same average value in both cases. Fig. 8 demonstrates that the current ripple is largely reduced in a low DC link voltage.

4.2 Direct compensation of dead time and voltage drop

Many studies have been performed to compensate for dead time and voltage drop [7-9]: methods have been proposed using an additional circuit, considering the mean voltage error produced during sampling period, and

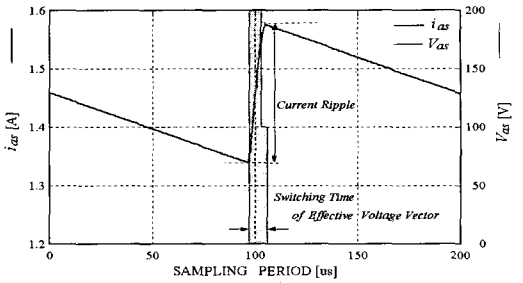

(a) V_{dc} = 300V

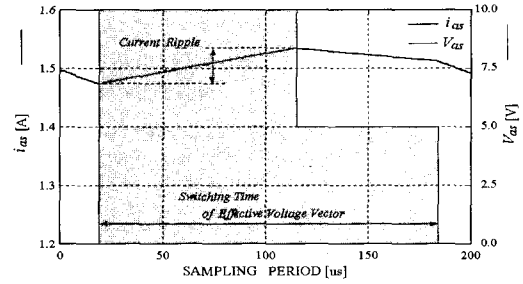

(b) V_{dc} = 15V

Fig. 8 Current ripples in DC link voltages of 300V and 15V

modifying switching time by using a feedback current controller. These methods require an additional circuit or controller or do not consider the effect of magnitude and direction of conducting current. The proposed algorithm using direct compensation for dead time and voltage drop is described here. Fig. 9 shows the switching pulse pattern including dead times. The switching pulse pattern used in this study produces two dead times for reducing the effect due to dead time, while a typical switching scheme shown in Fig. 3(b) produces three dead times. In Fig. 9, subscripts + and - mean upper and lower switches of inverter legs, respectively.

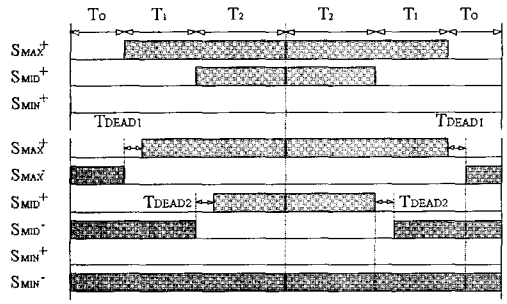

Fig. 9 Switching pulse pattern including dead time

The output voltage of the inverter in each switching state depends on the magnitude and direction of the conducting current. Fig. 10 shows the current path in each switching state. It has been assumed in Fig. 10 that $v_{as} = V_{MAX}^*$, $v_{bs} = V_{MID}^*$, $v_{cs} = V_{MIN}^*$, and the current i_{MID} in the phase of V_{MID}^* is positive. The voltage drop of the switching device is determined according to the

current path and the magnitude of the conducting current. Table 1 shows the voltage drop of the IGBT and diode used in this study.

The output voltage of the SVPWM-VSI and the modified switching time, including dead time and voltage drop, are described in the Appendix.

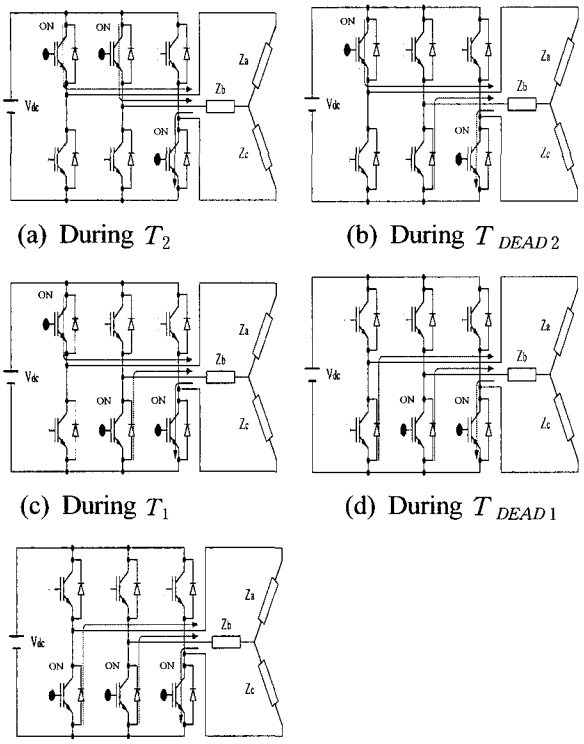

(a) During T_2 (b) During T_{DEAD2}

(c) During T_1 (d) During T_{DEAD1}

(e) During T_0

Fig. 10 Current path during $i_{MID} > 0$

Table 1 Forward voltage drop of IGBT and diode used in this study

Current [A]	1.0	3.0	5.0	7.0	9.0	11.0	13.0	15.0
V_{CE}[V], 25℃	0.886	1.191	1.377	1.517	1.631	1.729	1.815	1.893
V_{FD}[V], 25℃	0.933	1.162	1.376	1.584	1.791	1.996	2.200	2.403

5. Simulation

The simulation has been performed to verify the proposed strategy applied to a sensorless AC motor drive. In this study, a PMSM drive and a state observer based sensorless algorithm are used in the sensorless AC motor drive. A state observer based sensorless algorithm is a well-known senorless algorithm with good performance in the overall speed range [13,14]. Table 2 shows the specification of a PMSM used in the simulation and experimentation. Fig. 11 shows the speed and position responses in the speed command of 25 rpm and the fixed DC link voltage of 300 V, and Figs. 11(a) and 11(b) show the simulation without and with direct compensation for dead time and voltage drop, respectively.

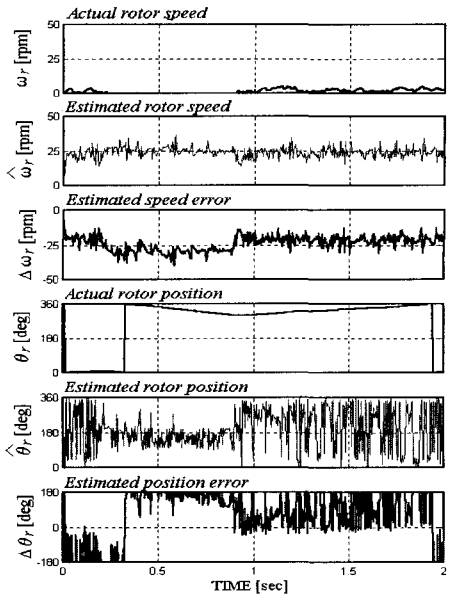

(a) Without dead time and voltage drop compensation

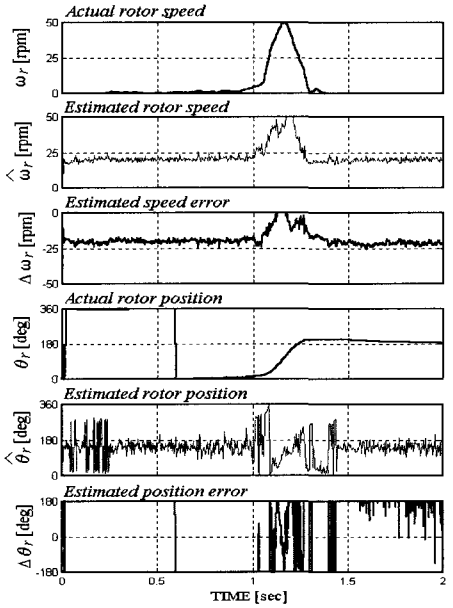

(b) With dead time and voltage drop compensation

Fig. 11 Speed and position responses in the fixed DC link voltage, 300V

Table 2 PMSM specification

the number of poles	8
rated output	600 W
rated current	5.8 A
emf constant	0.175 Vsec/rad
stator resistance	0.85 Ω
stator inductance	3.5 mH
connection	Y

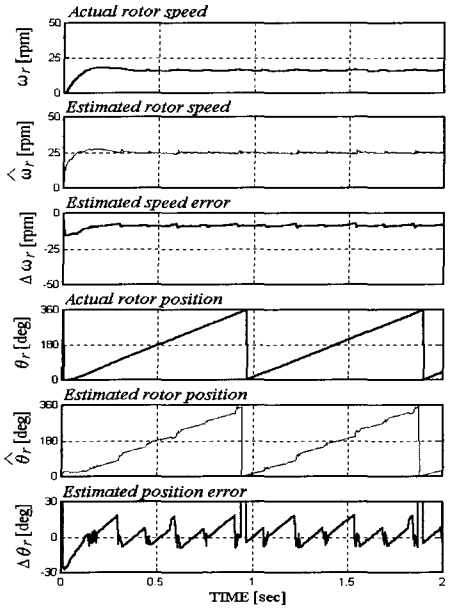

(a) Without dead time and voltage drop compensation

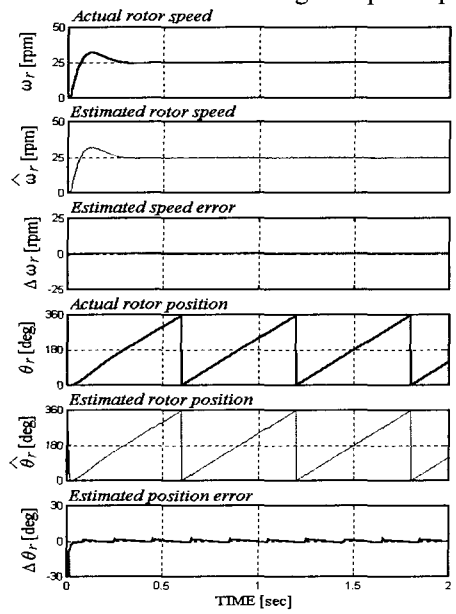

(b) With dead time and voltage drop compensation

Fig. 12 Speed and position responses in the variable DC link voltage

Fig. 12 shows the speed and position responses in the speed command of 25 rpm and the variable DC link voltage, and Figs. 12(a) and 12(b) show the simulation without and with direct compensation for dead time and voltage drop, respectively.

The simulation results show that the fixed DC link voltage of 300 V fails to bring a motor speed to the command speed of 25 rpm with both considering and not considering compensation for dead time and voltage drop, but the variable DC link voltage performs well even in a low speed. The direct compensation for dead time and voltage drop is well combined with the variable DC link voltage and reduces a steady state error in the speed and position responses as shown in Fig. 12.

6. Experiment and Discussions

The experiment has been performed in the sensorless PMSM drive, which is described in the simulation. The 80586 microprocessor system is used for digital processing of the proposed algorithm. Fig. 13 shows the experimental speed response in the speed command of 25 rpm and the fixed DC link voltage of 300 V, and Figs. 13(a) and 13(b) show the experimental results without and with direct compensation for dead time and voltage drop, respectively.

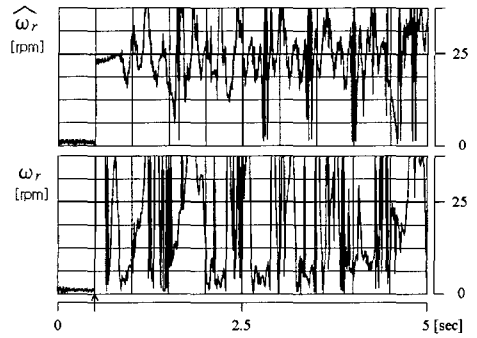

(a) Without dead time and voltage drop compensation

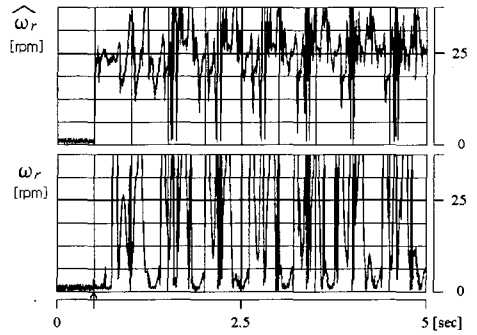

(b) With dead time and voltage drop compensation

Fig. 13 Experimental speed response in the fixed DC link voltage, 300 V

Fig. 14 shows the experimental speed response in the speed command of 25 rpm and the variable DC link voltage, and Figs. 14(a) and 14(b) show the experimental results without and with direct compensation for dead time and voltage drop, respectively. The experimental results also show that the fixed DC link voltage of 300 V fails to bring a motor speed to the command speed of 25 rpm with both considering and not considering a compensation for dead time and voltage drop, but the variable DC link voltage has good performance even in a low speed. The dead time and voltage drop compensation reduces a steady state error in the speed response.

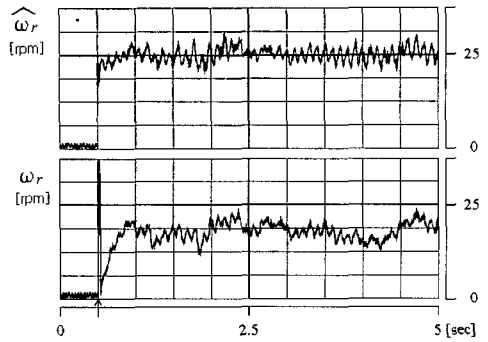

(a) Without dead time and voltage drop compensation

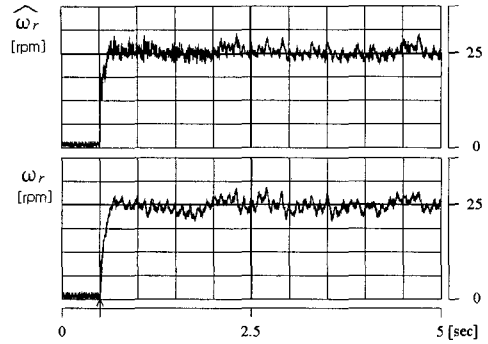

(b) With dead time and voltage drop compensation

Fig. 14 Experimental speed response in the variable DC link voltage

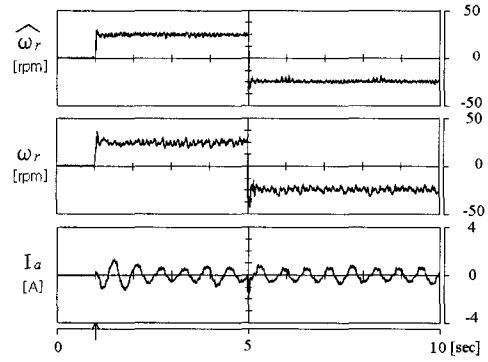

Fig. 15 Experimental speed response and current waveform in the bidirectional operation (±25rpm)

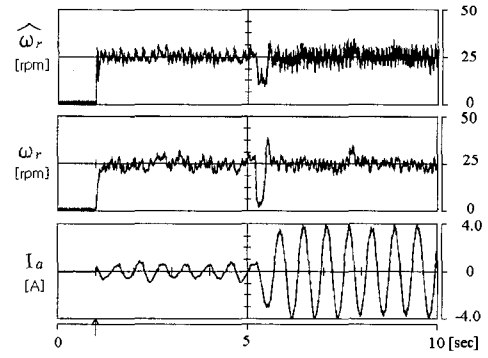

Fig. 16 Experimental speed response and current waveform in a load variation (25rpm, 0→5Nm)

Fig. 15 shows the experimental speed response and current waveform in the bidirectional operation of the speed command of ±25 rpm, obtained from the application of the proposed algorithm.

Fig. 16 shows the experimental speed response and current waveform in case the load torque of 4 Nm is applied in the middle of the operation of the speed command 25 rpm, obtained from the application of the proposed algorithm.

7. Conclusions

This paper investigates a novel high-performance strategy for a sensorless AC motor drive overcoming the poor resolution of the SVPWM-VSI in the low speed range of a motor and a voltage distortion due to dead time and voltage drop. In the proposed strategy, the output voltage of the SVPWM-VSI is more exactly obtained through the variable DC link voltage and the direct compensation for dead time and voltage drop. The variable DC link voltage largely improves resolution of the inverter output voltage, especially in the low speed range of a motor. The direct compensation for dead time and voltage drop directly calculates the duration of the switching voltage vector without modification of the reference voltage, and needs no additional circuits. In addition, the variable DC link voltage has an advantage of reducing a current ripple produced in the SVPWM-VSI.

Simulation and experimental results show that the variable DC link voltage indicates good performance even in the low speed range where the fixed DC link voltage fails to control the motor, and the direct compensation for dead time and voltage drop is satisfactorily applied and reduces a steady state error.

Appendix

The output voltage of the SVPWM-VSI including the dead time and voltage drop described in Section 3, may be written as

$$\begin{aligned} V_{MAX} =& \left(\frac{1}{3}V_{dc} - V_{CE}(i_{MAX}) + Voff_{T2}\right)\frac{(T_2 + T_{OFF})}{T_S} \\ &+ \left(\frac{1}{2}V_{dc} - V_{CE}(i_{MAX}) + Voff_{TD2}\right)\frac{(T_{DEAD} + T_{ON} - T_{OFF})}{T_S} \\ &+ \left(\frac{2}{3}V_{dc} - V_{CE}(i_{MAX}) + Voff_{T1}\right)\frac{(T_1 - T_{DEAD} - T_{ON} + T_{OFF})}{T_S} \\ &- (V_{FD}(i_{MAX}) - Voff_{TD1})\frac{(T_{DEAD} - T_{OFF} + T_{ON})}{T_S} \\ &- (V_{FD}(i_{MAX}) - Voff_{TO})\frac{(T_O - T_{DEAD} - T_{ON})}{T_S} \end{aligned} \quad \text{(A1)}$$

$$V_{MID} = \left(\frac{1}{3}V_{dc} - V_{CE}(i_{MID}) + Voff_{T2}\right)\frac{(T_2 + T_{OFF})}{T_S} - (V_{FD}(i_{MID}) - Voff_{TD2})\frac{(T_{DEAD} + T_{ON} - T_{OFF})}{T_S} - \left(\frac{1}{3}V_{dc} + V_{FD}(i_{MID}) - Voff_{T1}\right)\frac{(T_1 - T_{DEAD} - T_{ON} + T_{OFF})}{T_S} - (V_{FD}(i_{MID}) - Voff_{TD1})\frac{(T_{DEAD} - T_{OFF} + T_{ON})}{T_S} - (V_{FD}(i_{MID}) - Voff_{TO})\frac{(T_O - T_{DEAD} - T_{ON})}{T_S} \quad \text{(A2)}$$

$$V_{MIN} = \left(-\frac{2}{3}V_{dc} + V_{CE}(i_{MIN}) + Voff_{T2}\right)\frac{(T_2 + T_{OFF})}{T_S} - \left(\frac{1}{2}V_{dc} - V_{CE}(i_{MIN}) - Voff_{TD2}\right)\frac{(T_{DEAD} + T_{ON} - T_{OFF})}{T_S} - \left(\frac{1}{3}V_{dc} - V_{CE}(i_{MIN}) - Voff_{T1}\right)\frac{(T_1 - T_{DEAD} - T_{ON} + T_{OFF})}{T_S} + (V_{CE}(i_{MIN}) + Voff_{TD1})\frac{(T_{DEAD} - T_{OFF} + T_{ON})}{T_S} + (V_{CE}(i_{MIN}) + Voff_{TO})\frac{(T_O - T_{DEAD} - T_{ON})}{T_S} \quad \text{(A3)}$$

where

$$Voff_{T2} = \frac{V_{CE}(i_{MAX}) + V_{CE}(i_{MID}) - V_{CE}(i_{MIN})}{3}$$

$$Voff_{TD2} = \frac{V_{CE}(i_{MAX}) + V_{FD}(i_{MID}) - V_{CE}(i_{MIN})}{3}$$

$$Voff_{TD1} = \frac{V_{FD}(i_{MAX}) + V_{FD}(i_{MID}) - V_{CE}(i_{MIN})}{3}$$

$$Voff_{T1} = Voff_{TD2}, \quad Voff_{TO} = Voff_{TD1}$$

T_{ON}, T_{OFF} is the turn-on and turn-off time of the switching device, T_{DEAD} is the dead time, $V_{CE}(i_{MAX})$, $V_{CE}(i_{MID})$, $V_{CE}(i_{MIN})$ is the voltage drop of switching device, and $V_{FD}(i_{MAX})$, $V_{FD}(i_{MID})$, $V_{FD}(i_{MIN})$ is the voltage drop of diode.

From (A1)-(A3), the modified switching time considering dead time and voltage drop becomes the solution of the following equations in which one equation is redundant.

$$A_{11} \cdot T_2 + A_{21} \cdot T_1 = y_1 \quad \text{(A4)}$$

$$A_{12} \cdot T_2 + A_{22} \cdot T_1 = y_2 \quad \text{(A5)}$$

$$A_{13} \cdot T_2 + A_{23} \cdot T_1 = y_3 \quad \text{(A6)}$$

where

$$A_{11} = \frac{1}{3}V_{dc} - V_{CE}(i_{MAX}) + V_{FD}(i_{MAX}) + Voff_{T2} - Voff_{TO}$$

$$A_{21} = \frac{2}{3}V_{dc} - V_{CE}(i_{MAX}) + V_{FD}(i_{MAX}) + Voff_{T1} - Voff_{TO}$$

$$A_{12} = \frac{1}{3}V_{dc} - V_{CE}(i_{MID}) + V_{FD}(i_{MID}) + Voff_{T2} - Voff_{TO}$$

$$A_{22} = -\frac{1}{3}V_{dc} + Voff_{T1} - Voff_{TO}$$

$$A_{13} = -\frac{2}{3}V_{dc} + Voff_{T2} - Voff_{TO}$$

$$A_{23} = -\frac{1}{3}V_{dc} + Voff_{T1} - Voff_{TO}$$

$$y_1 = T_S \cdot (V_{MAX}^* + V_{FD}(i_{MAX}) - Voff_{TO}) + T_{DEAD} \cdot (V_{dc}/6) + T_{ON} \cdot (V_{dc}/6) - T_{OFF} \cdot (V_{dc}/2 - V_{CE}(i_{MAX}) + V_{FD}(i_{MAX}) + Voff_{T2} - Voff_{TO})$$

$$y_2 = T_S \cdot (V_{MID}^* + V_{FD}(i_{MID}) - Voff_{TO}) - T_{DEAD} \cdot (V_{dc}/3) - T_{ON} \cdot (V_{dc}/3) + T_{OFF} \cdot (V_{CE}(i_{MID}) - V_{FD}(i_{MID}) - Voff_{T2} + Voff_{TO})$$

$$y_3 = T_S \cdot (V_{MIN}^* - V_{CE}(i_{MIN}) - Voff_{TO}) + T_{DEAD} \cdot (V_{dc}/6) + T_{ON} \cdot (V_{dc}/6) + T_{OFF} \cdot (V_{dc}/2 - Voff_{T2} + Voff_{TO})$$

References

[1] K. Rajashekara, A. Kawamura, and K. Matsuse, *Sensorless Control of AC Motor Drives*, IEEE Press, 1996.

[2] J. Holtz, "State of the Art of Controlled AC Drives Without Speed Sensors," Int. J. Electronics, vol.80, no.2, pp.249-263, 1996.

[3] P. Vas, *Sensorless Vector and Direct Torque Control*, Oxford Univ. Press, 1998.

[4] H. W. Van der Broeck and H. C. Skudelny, "Analysis and Realization of a Pulse Width Modulator Based on Voltage Space Vectors," IEEE, IA-24, no.1, pp.142-150, 1988.

[5] F. Jenni and D. Wueest, "The Optimization Parameters of Space Vector Modulation," Power Electronics and Applications, 5th European Conference, vol.4, pp.376-381, 1993.

[6] Y. S. Lai and S. R. Bowes, "A New Suboptimal Pulse-Width Modulation Technique for Per-Phase Modulation and Space Vector Modulation," IEEE, EC-12, no.4, pp.310-316, 1997.

[7] Y. Murai, T. Watanabe, and H. Iwasaki, "Waveform Distortion and Correction Circuit for PWM Inverters with Switching Lag-Times," IEEE, IA-23, no.5, pp. 881-886, 1987.

[8] J. W. Choi and S. K. Sul, "Inverter Output Voltage Synthesis Using Novel Dead Time Compensation,"

IEEE, PE-11, no.2, pp.221-227, 1996.
[9] A. R, Muñoz and T. A. Lipo, "On-Line Dead-Time Compensation Technique for Open-Loop PWM-VSI Drives," IEEE, PE-14, no.4, pp.683-689, 1999.
[10] D. H. Lee and Y. A. Kwon, "Improved Performance of SVPWM Inverter Based on Novel Dead Time and Voltage Drop Compensation," KIEE, vol.49, no.9, pp.618-625, 2000.
[11] N. Mohan, T. M. Undeland, and W. P. Robbins, *Power Electronics*, John Wiley & Sons, 1989.
[12] A. I. Pressman, *Switching Power Supply Design*, McGraw-Hill, 1998.

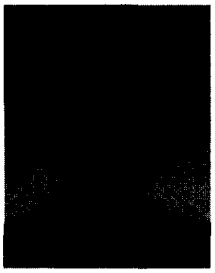

Dong-Hee Lee received the B.S., M.S., and Ph.D. degrees in Electrical Engineering from Pusan National University in 1996, 1998, and 2001, respectively. His research interests include motor drive, and power electronics.

[13] R. B. Sepe and J. H. Lang, "Real-Time Observer-Based Control of a Permanent-Magnet Synchronous Motor without Mechanical Sensors," IEEE, IA-28, no.6, pp.1345-1352, 1992.
[14] J. Solsona, M. I. Valla, and C. Muravchik, "A Nonlinear Reduced Order Observer for Permanent Magnet Synchronous Motors," IEEE, IE-43, no.4, pp.492-497, 1996.

Young-Ahn Kwon received the B.S, M.S., and Ph.D. degrees in Electrical Engineering from Seoul National University in 1978, 1983, and 1986, respectively. He is currently a professor of the School of Electrical Engineering at Pusan National University. His research interests include electric machinery, power electronics, and control.
E-mail: yakwon@pusan.ac.kr